

Resonant gravitational wave antennas for stochastic background measurements

Pia Astone[†], G V Pallottino[‡] and G Pizzella[§]

[†] INFN sezione Roma 1, P A Moro 2, 00185, Rome, Italy

[‡] University of Rome ‘La Sapienza’ and INFN sezione Roma 1, P A Moro 2, 00185, Rome, Italy

[§] University of Rome ‘Tor Vergata’ and INFN Laboratori Nazionali di Frascati, Via E Fermi 40, 00044, Frascati, Italy

Received 11 July 1996, in final form 10 April 1997

Abstract. The sensitivity of a resonant gravitational wave (GW) antenna is calculated in terms of spectral density and frequency bandwidth. For a quantum-limited detector the bandwidth might reach values greater than 100 Hz, with a sensitivity to bursts of $h = 3 \times 10^{-21}$ (SNR = 1). The spectral amplitude sensitivity for the Nautilus detector has been measured to be $7 \times 10^{-22} \text{ Hz}^{-1/2}$ and its target value is $7 \times 10^{-23} \text{ Hz}^{-1/2}$. Using two near-Nautilus detectors the GW stochastic background can be measured with a sensitivity, with respect to the critical density, of a few 10^{-5} for an integration time of one year, as shown by simulations.

PACS number: 0480N, 9880

1. Introduction

At the beginning of the experimental search for gravitational waves (GWs) the main scientific goal was to detect GW bursts due to gravitational collapses. Subsequently, various detectors were developed with the purpose of also looking for other types of GW, such as those due to pulsars or to the coalescence of binary systems [1]. All these detectors, constructed or planned, cover the frequency range 10 Hz–10 kHz. Another type of GW considered by various authors is the stochastic background. This is one of the most interesting, as it might give information on the very early stages of the Universe and its formation. Several sources of stochastic background have been considered in the past few years [1]. We recall the effect of the superposition of waves generated by pulsars and of bursts due to gravitational collapses and to the coalescence of binary systems. Considerations based on nucleosynthesis put an upper limit on the stochastic GW, which is usually expressed in terms of the ratio Ω of the GW energy density to the critical density needed for a closed universe ($\Omega \leq 10^{-5}$). Considering a GW with a dimensionless amplitude h , the general relationship between the GW density $\Omega(f) = d\Omega/d(\ln f)$ and the power spectrum $S_h(f)$ of h (in Hz^{-1}) is

$$\Omega(f) = \frac{4\pi^2}{3} \frac{f^3}{H^2} S_h(f) = 1.25 \times 10^{45} \left(\frac{f}{1 \text{ kHz}} \right)^3 \left(\frac{100 \text{ km s}^{-1} \text{ Mpc}^{-1}}{H} \right)^2 S_h(f) \quad (1)$$

where H is the Hubble constant.

Recently, a new source based on the string theory of matter has been proposed [2], which predicts relict GWs, the density of which $\Omega(f)$ increases with frequency f to the third power. In such a case $S_h(f)$ would be independent of the frequency. In fact, the previous models of stochastic background tend to predict GWs in the frequency range below 1 Hz, less than the operating frequency of the detectors already in operation (resonant bars) or entering into operation in the next four to five years (long-arm interferometers).

Resonant detectors have been developed since 1960 and large cryogenic bars were put into continuous operation in 1990 [3–5]. In this paper we have decided to re-examine the sensitivity of resonant bars to the various types of GW, putting special emphasis on the stochastic background.

2. The resonant detector

We have re-examined the sensitivity of a resonant bar to GW in a simple form, although sometimes with approximations only aimed to help clarity. As an initial model for these detectors, we consider the simplest resonant antenna, a cylinder of high- Q material, coupled to a non-resonant transducer followed by a very low-noise electronic amplifier. In practice, the detectors currently operating use resonant transducers (and therefore there are two modes coupled to the gravitational field) (see section 5) in order to obtain high coupling. For a non-resonant transducer the equation for the end bar displacement ξ is

$$\ddot{\xi} + \frac{\omega_0}{Q}\dot{\xi} + \omega_0^2\xi = \frac{F}{m} \quad (2)$$

where F is the applied force, m the oscillator reduced mass (for a cylinder with $m = M/2$), $\omega_0 = 2\pi f_0$ is the angular resonance frequency and Q is the merit factor. Here we consider only noise of fundamental origin, which derives from two contributions: the thermal (Brownian) noise of the basic detector and the electronic noise of the readout system. By referring the overall noise to the displacement of the bar ends, we obtain [6] the noise power spectrum:

$$S_\xi^n(f) = \frac{S_F}{(2\pi)^4 m^2} \frac{1 + \Gamma[Q^2(1 - (f/f_0)^2)^2 + (f/f_0)^2]}{(f^2 - f_0^2)^2 + (ff_0/Q)^2} \quad (3)$$

with

$$S_F = \frac{2\omega_0}{Q}mkT_e \quad (4)$$

where T_e is the equivalent temperature of the detector that includes the heating effect (back-action) due to the electronic amplifier, and Γ (usually $\Gamma \ll 1$) is the spectral ratio between electronic and Brownian noise [7].

When a gravitational wave with amplitude h and optimum polarization impinges perpendicularly to the bar axis of length L , the bar displacement corresponds [8] to the action of a force $F = (2/\pi^2)mL\ddot{h}$. For a GW excitation with power spectrum $S_h(f)$, the spectrum of the corresponding bar end displacement is

$$S_\xi(f) = \frac{4L^2 f^4 S_h(f)}{\pi^4} \frac{1}{(f^2 - f_0^2)^2 + (ff_0/Q)^2}. \quad (5)$$

We notice that the power spectrum of the bar displacement for a constant spectrum of GWs is similar to that due to the action of the Brownian force. Therefore, if only the Brownian

noise were present ($\Gamma = 0$), we would have an infinite bandwidth, in terms of signal-to-noise ratio (SNR). By taking the ratio of the noise spectrum (3) and the signal spectrum (5) we obtain the signal-to-noise ratio (SNR)

$$\text{SNR}(f) = \frac{S_\xi(f)}{S_\xi^n(f)} = \frac{64L^2 f^4 m^2 S_h(f)}{S_F} \frac{1}{1 + \Gamma[Q^2(1 - (f/f_0)^2)^2 + (f/f_0)^2]}. \quad (6)$$

By equating to unity the above ratio we obtain the GW spectrum detectable with $\text{SNR} = 1$, that is the detector noise spectrum referred to the input

$$S_h(f) = \frac{\pi}{8} \frac{kT_e}{MQL^2} \frac{f_0}{f^4} (1 + \Gamma[Q^2(1 - (f/f_0)^2)^2 + (f/f_0)^2]). \quad (7)$$

At the resonance f_0 we have ($\Gamma \ll 1$)

$$S_h(f_0) = \frac{\pi}{8} \frac{kT_e}{MQL^2} \frac{1}{f_0^3} = \frac{\pi kT_e}{\rho v^3 S Q} \quad (8)$$

where ρ is the density of the material, v the sound velocity, S the cross section of the cylinder and we have used the relation

$$f_0 = v/(2L). \quad (9)$$

We remark that for a cylinder $S_h(f_0)$ does not depend on its resonance frequency but on the size of the bar (section) and some characteristics of the material (ρ, v). We also notice that, for a given resonance frequency f_0 , the best spectral sensitivity, obtained at the resonance, only depends on the temperature T , on the mass M and on the quality factor Q of the detector, provided $T \simeq T_e$, that is the coupling between bar and read-out system is sufficiently small. Note that those conditions are rather different from that required for optimum pulse sensitivity (see later).

An example of the sensitivity expressed in terms of the spectral amplitude is given in figure 1 where we have used the target parameters for the Nautilus antenna. The bandwidth,

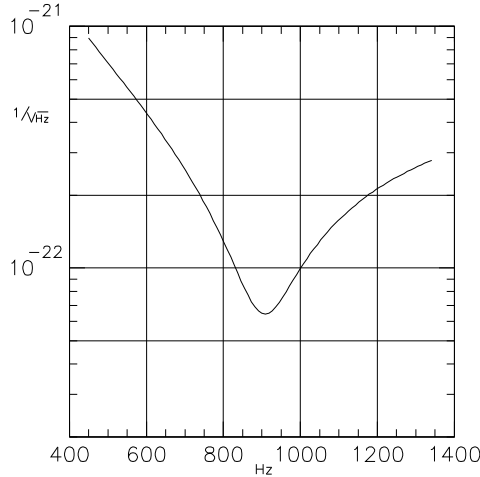


Figure 1. Spectral amplitude for a resonant antenna with the following characteristics: $f_0 = 900$ Hz, $Q = 8.5 \times 10^6$, $T_e = 0.1$ K, $L = 3$ m, $M = 2300$ kg, $T_{\text{eff}} = 3 \times 10^{-7}$ K, $\Gamma = 7 \times 10^{-13}$.

in this example estimated at the half-height of the power spectrum, is $\Delta f = 130$ Hz. This quantity is given, in general, by

$$\Delta f = \frac{f_0}{Q} \frac{1}{\sqrt{\Gamma}} \quad (10)$$

which is obtained [7] from the spectrum (7). Again we notice that if the amplifier were noiseless ($\Gamma = 0$) the bandwidth would be infinite.

3. Sensitivity for deterministic signals

3.1. Short bursts

We now apply the optimum filter for detecting short signals. It can be shown [9] that the SNR for a gravitational wave signal $h(t)$ with Fourier transform $H(f)$ is given by

$$\text{SNR} = \int_{-\infty}^{+\infty} \frac{|H(f)|^2}{S_h(f)} df. \quad (11)$$

We solve (11) with $\text{SNR} = 1$ by noticing that S_h has a minimum around the resonance (see figure 1) and that, for a short burst of duration $< 1/f_0$, $H(f) = H_0$. We obtain

$$H_0^2 = \frac{S_h(f_0)}{2\pi \Delta f} \quad (12)$$

with Δf given by (10). The factor of 2π has been introduced because we need the equivalent frequency bandwidth for a two-sided spectrum. Introducing (8) and (9) we get

$$H_0 = \frac{L}{2v^2} \sqrt{\frac{kT_{\text{eff}}}{M}} \quad (13)$$

where

$$T_{\text{eff}} = 4T_e \sqrt{\Gamma} \quad (14)$$

is the effective temperature [10] which represents the minimum energy change of the detector (innovation), expressed in kelvin units, that can be detected with $\text{SNR} = 1$ after filtering the data.

From equation (13) one can get the value of h for a short burst assuming a duration of 1 ms and putting, roughly, $h = H_0/0.001$. The corresponding h value is often referred to as the conventional amplitude for a GW burst.

By substituting equation (14) into equation (10), the bandwidth can be recast in the form

$$\Delta f = \frac{f_0}{Q} \frac{4T_e}{T_{\text{eff}}} \quad (15)$$

that is, as a product of the mechanical bandwidth f_0/Q and of the SNR improvement obtained by filtering the data for burst detection.

3.2. Monochromatic waves

For a total measuring time t_m we could detect, with $\text{SNR} = 1$, a monochromatic GW with strength [11]

$$h = \sqrt{\frac{2S_h(f)}{t_m}} = \sqrt{\frac{2\pi^2 k T_e}{M Q v^2 \omega_0 t_m}} \quad (16)$$

where the second equality is valid only at the resonance (the factor of 2 takes care of the fact that S_h is two-sided). This formula can be derived as follows: for a total measuring time t_m a monochromatic wave of amplitude h_0 is just like a wavepacket of duration t_m , whose Fourier transform has a maximum $h_0 t_m/2$. Thus from (11) we get

$$\text{SNR} = \frac{h_0^2 t_m^2/4}{S_h(\omega_0) t_m} \frac{2}{1} \quad (17)$$

which gives (16) for $\text{SNR} = 1$.

In the practical case it is not possible to calculate the Fourier spectrum of the experimental data over the entire period of measurement t_m , because of the change in frequency due to the Doppler effect for a monochromatic wave. It is then necessary to divide the period t_m into n subperiods of length $\Delta t = t_m/n$. For the search of a monochromatic wave we have to consider two cases:

(i) The wave frequency is exactly known. In this case we can combine the n Fourier spectra into one single spectrum, taking into account the phase of the signal. The final spectrum then has the same characteristics of the spectrum over the entire period t_m and equation (16) still applies.

(ii) The exact frequency is unknown. In this case when we combine the n spectra we lose the information on the phase. The result is that the final combined spectrum over the entire period has a larger variance. The left-hand side of equation (16) has to be changed to

$$h = \sqrt{\frac{2S_h(f)}{\sqrt{\Delta t} t_m}} = \sqrt{\frac{2S_h(f)}{t_m}} \sqrt{n}. \quad (18)$$

4. Stochastic waves

Using one detector, the measurement of the noise spectrum given by equation (7) (see also figure 1) only provides an upper limit for the GW stochastic background spectrum. To improve the estimation of this spectrum one has to cross-correlate the output signals of two (or more) antennas.

Until now the limits to the stochastic background, near 1 kHz, have been set using bar detectors in Glasgow [12, 13], interferometers (Garching–Glasgow) [14] and cryogenic bar detectors [15].

Our considerations in this paper refer to the case of two antennas located very near one another and parallel. The case of two non-parallel antennas located at a distance R has been considered by Michelson [16]. Let us consider two antennas with transfer functions $T_1(f)$ and $T_2(f)$, displacements ξ_1 and ξ_2 and spectral densities $S_1(f)$ and $S_2(f)$: the displacement cross-correlation function

$$R_{\xi_1 \xi_2}(\tau) = \int \xi_1(t) \xi_2(t + \tau) dt \quad (19)$$

only depends on the common excitation of the detectors, due to the GW stochastic background spectrum S_{GW} acting on both of them and is not affected by the noises acting independently on the two detectors. Note that the above result only holds if the cross-correlation function is evaluated over an infinite time. Otherwise there is a residual statistical error, due to the noise, which decreases with the duration of the observation period.

The Fourier transform of equation (19) represents the displacement cross spectrum. This is a complex quantity $S_{12}(f) = C_{12}(f) - jQ_{12}(f)$. The real part shows the correlation at zero time delay and, referred to the detector input (multiplying it by $T_1 T_2$ times $4L^2/\pi^4$),

gives an estimate of the gravitational background S_{GW} . The estimate, obtained over a finite observation time t_m , has a statistical error. It can be shown [17] that the standard deviation of each sample of the spectrum is

$$\delta C_{12}(f) \leq \frac{\sqrt{S_{1h}(f)S_{2h}(f)}}{\sqrt{t_m} \delta f}; \quad \delta Q_{12}(f) \leq \frac{\sqrt{S_{1h}(f)S_{2h}(f)}}{\sqrt{t_m} \delta f} \quad (20)$$

where t_m is the total measuring time and δf is the frequency step in the power spectrum.

From figure 1 we get the obvious result that, for resonant detectors, the error is smallest at the resonances. If the resonances of the two detectors coincide, the error is even smaller. In practice, the best policy is to have two detectors with the same resonance and bandwidth. If one bandwidth is smaller than the other one then the smallest error occurs in the frequency region overlapping the smallest bandwidth. Note, however, that according to equation (20) there is no improvement, besides an obvious increase of confidence, in using two detectors instead of one, when the frequency step δf of the spectrum is chosen to be equal to $1/t_m$. In this case the statistical improvement factor $\sqrt{\delta f t_m}$ reduces in fact to unity and the sensitivity, for two identical detectors, coincides with that of a single detector, given by equation (7).

If the background spectrum is expected [2] to be approximately constant over a few Hz or a few tens of Hz near the resonances of the detector, we can shift our attention from a detailed, and statistically expensive, spectral estimation to estimating its intensity over a spectral interval Df much larger than the spectral step δf , properly chosen in the region of maximum sensitivity of the detectors, as discussed above, but such that the two spectral densities are quite flat. The uncertainty of this estimate is obtained as follows from equation (20):

$$\delta S_{\text{GW}}(f) \leq \frac{\sqrt{(1/Df) \int_{Df} S_{1h}(f)S_{2h}(f) df}}{\sqrt{t_m} Df} \quad (21)$$

where Df is the smallest of the two overlapping bandwidths.

For the search for a stochastic background, however, one expects at first just to find upper limits. In this case the estimated spectrum S_{GW} will be zero with a standard error given by (21) and the overall sensitivity of this cross-correlation experiment, considering an observation bandwidth Df , will be again given by equation (21).

5. Calculation of the sensitivity for stochastic waves by means of data simulated for the antenna Nautilus

In order to verify that the resonant antennas behave as expected, at least in principle, we have performed simulations for the ultracryogenic antennas [18–20]. We recall that Nautilus is an aluminium bar with length $L = 3$ m and mass $M = 2300$ kg. The antenna is equipped with a capacitive resonant mushroom [19] transducer followed by a DC SQUID amplifier. Because of the resonant transducer there are two resonant modes at frequencies of about $f_- = 905$ Hz and $f_+ = 921$ Hz.

In the case of a detector with a resonant transducer we can still use the previous formulae valid for a non-resonant transducer [21], provided we also take into account the stochastic force acting on the transducer oscillator (corresponding to that represented by the spectrum (4) for the bar oscillator). If the transducer is well tuned to the bar the effect of this additional force is equivalent to double the force spectrum (4). We can therefore use equations (3),

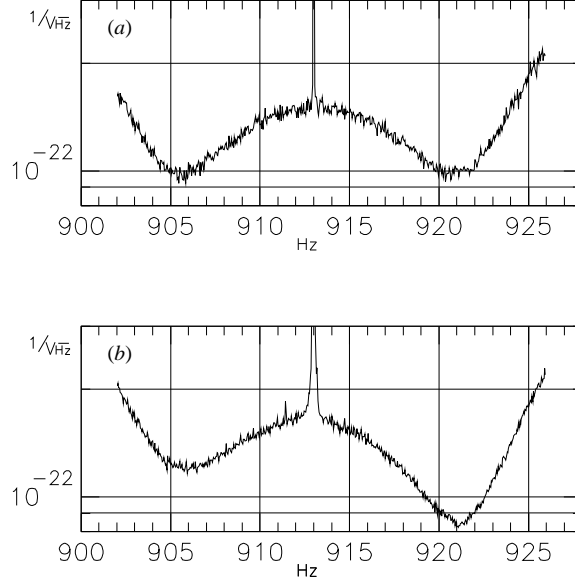


Figure 2. Spectral amplitude sensitivity versus frequency expected for the Nautilus detector in the year 2000, as obtained by simulation: (a) the electromechanical transducer is well coupled to the bar; (b) the transducer is only partially coupled to the bar.

(7) and (8) near f_- and f_+ , provided we rewrite equation (4) as

$$S_{f_{\pm}} = \frac{4\omega_{\pm}}{Q} m k T_e. \quad (22)$$

This means that the final spectral sensitivity is reduced by a factor of 2. Equations (3), (7) and (8) can be also used for any arbitrary tuning of the transducer. In such a case the equivalent force spectra for the two modes are different: we have

$$S_{f_-} = \frac{S_F}{a_-} \quad \text{and} \quad S_{f_+} = \frac{S_F}{a_+} \quad \text{with} \quad 0 \leq a_{\pm} \leq 1 \quad \text{and} \quad a_- + a_+ = 1. \quad (23)$$

This means that at one mode we can obtain the full spectral sensitivity at the expense of a reduced sensitivity for the other mode.

A simulation of the expected spectral amplitude sensitivity $\tilde{h} = \sqrt{S_h}$ for Nautilus is shown in figure 2. In figure 2(a) we have considered $a_+ = a_- = 0.5$; the other parameters are those used in figure 1, except for the frequency bandwidth which is taken to be equal to 6 Hz, which we plan to reach it in the near future. As expected from (8) and (23) at the two resonances we get $\tilde{h} = 6.5 \times 10^{-23} / \sqrt{0.5} = 9.2 \times 10^{-23} \text{ Hz}^{-1/2}$. A similar simulation is shown in figure 2(b), with the same parameters except that $a_- = 0.33$ and $a_+ = 0.67$, corresponding to a looser tuning of the transducer to the bar (here the bar and transducer resonance frequencies differ by about 5 Hz). We notice, as expected, a worse sensitivity at the mode f_- , in agreement with the calculated $\tilde{h} = 6.5 \times 10^{-23} / \sqrt{0.33} = 1.13 \times 10^{-22} \text{ Hz}^{-1/2}$ and a better sensitivity at the mode f_+ , $\tilde{h} = 6.5 \times 10^{-23} / \sqrt{0.67} = 7.9 \times 10^{-23} \text{ Hz}^{-1/2}$. The statistical fluctuation is given by equation (20); in the case of figure 3 with $\sqrt{I_m} \delta \bar{f} = 8.94$, we calculate a standard deviation at f_+ of $\delta \tilde{h} = 4.4 \times 10^{-24} \text{ Hz}^{-1/2}$. This error takes into account the difference between the

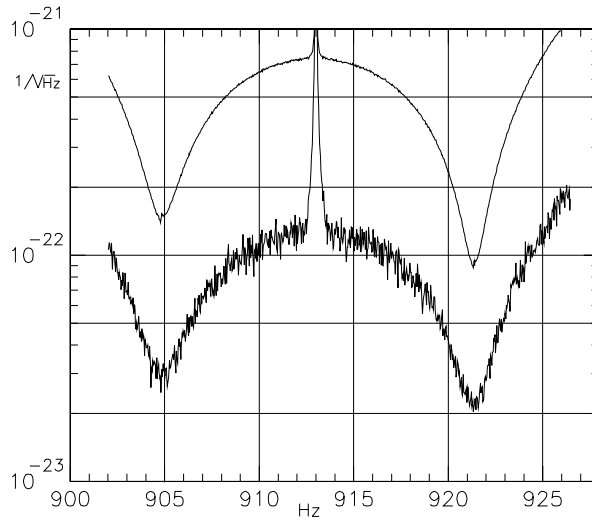


Figure 3. The lower curve shows the result of a simulated cross-correlation of two identical near-Nautilus detectors (the upper curve shows for reference the spectral amplitude sensitivity for a single detector). We note the improvement in sensitivity by a factor of $(t_m \delta f)^{1/4} = 4.6$, as expected ($t_m = 36$ h, $\delta f = 3.35$ mHz).

expected value, $7.9 \times 10^{-23} \text{ Hz}^{-1/2}$, and the value found by simulation of $8.2 \times 10^{-23} \text{ Hz}^{-1/2}$ shown in figure 2(b).

Let us now consider two identical Nautilus antennas located in parallel at a distance which is small compared with the GW wavelength. We calculate the cross-correlation between the two antennas, from which we derive the estimation of the spectrum S_{GW} . In the absence of a GW stochastic background S_{GW} should turn out to be null. The standard deviation is again obtained by means of equation (20), depending on the measuring time t_m and on the frequency step δf .

The result of the cross-correlation is shown in figure 3. Here we have plotted the simulated spectral amplitude $\sqrt{S_h(f)}$ for one antenna only (upper curve) with the parameters of figure 2 and the square root of the modulus of the cross spectrum of two identical antennas (lower curve). Since there is no correlation between the two detectors, we expect a null result at all frequencies, with a certain statistical error. According to equation (20) the statistical error can be obtained by the upper curve divided by $\sqrt{\sqrt{t_m \delta f}} = 4.56$. This is exactly the result we obtain by the cross-correlation, as shown by the lower curve in the figure.

To show a possible correlation between the two detectors it might be convenient to use the coherence function between the two spectra $S_1(f)$ and $S_2(f)$, defined as

$$\gamma_0(f) = S_{12}(f) / \sqrt{S_1(f)S_2(f)}. \quad (24)$$

This function has the property that $0 \leq |\gamma_0| \leq 1$ and is equal to 0 for a null correlation and to 1 for total correlation.

The standard deviations of $\gamma_0(f) = \text{Re}[\gamma_0(f)] + j \text{Im}[\gamma_0(f)]$ are

$$\delta \text{Re}[\gamma_0] \leq \frac{1 + |\text{Re}[\gamma_0]|}{\sqrt{t_m \delta f}}; \quad \delta \text{Im}[\gamma_0] \leq \frac{1 + |\text{Im}[\gamma_0]|}{\sqrt{t_m \delta f}}. \quad (25)$$

In the case of the cross-correlation of figure 3 we obtain the results shown in figure 4 for the real and imaginary part of $\gamma_0(f)$ in the frequency window 914–915 Hz.

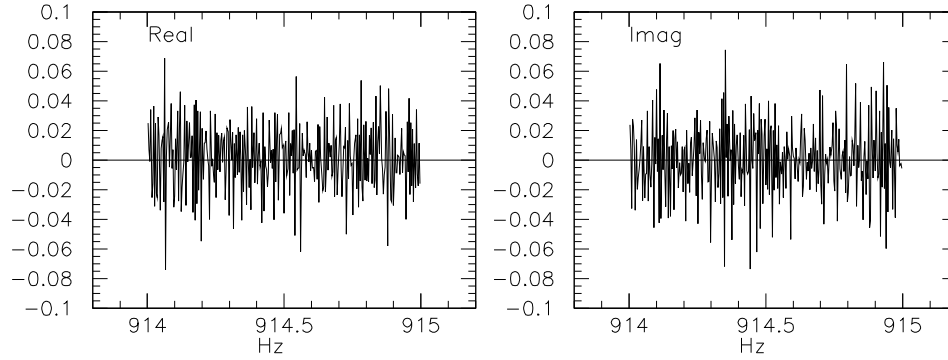


Figure 4. Simulation. Real and imaginary part of the coherence function $\gamma_0(f)$, in the bandwidth 914.0–915.0 Hz (297 samples), in the absence of correlation.

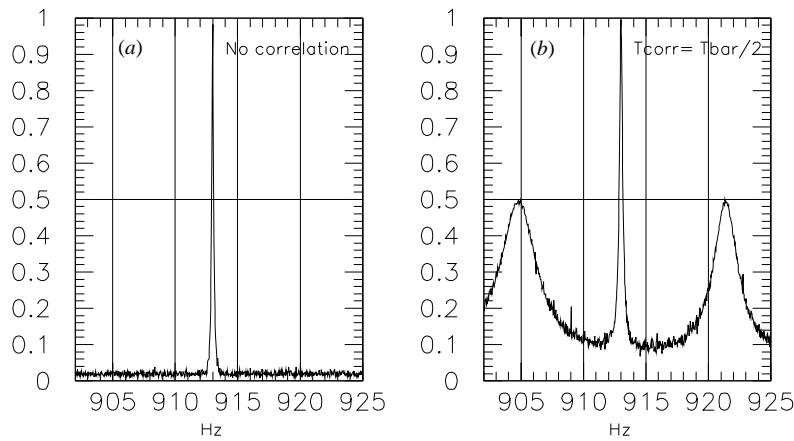


Figure 5. Simulation. Modulus of the real part of the coherence function: (a) without correlation (the peak is due to the calibration signal); (b) with partial correlation ($T_{\text{corr}} = T_{\text{bar}}/2$).

We notice that both parts fluctuate near zero, as expected, with average values 1.4×10^{-3} and 2.1×10^{-4} . The statistical errors on the averages from the simulated values are 1.3×10^{-3} and 1.4×10^{-3} , respectively, indicating that the two averages are indeed in agreement with null values. The standard deviation obtained from equation (25) is, with $t_m = 36$ h and $Df = 1$ Hz, $1/\sqrt{36 \times 3600 \text{ s} \times 1 \text{ Hz}} = 2.8 \times 10^{-3}$, in agreement with the standard deviations obtained by the simulation, because the standard deviation given by (25) represents only an upper limit of the actual standard deviation.

We have also performed simulation experiments for two identical antennas both driven by a common stochastic background signal with constant spectrum in the frequency region of interest, for various values of intensity of the spectrum.

The results of the cross-correlation are reported in terms of the correlation parameter T_{corr} (K). Using equations (8) and (24) the coherence function at the resonance frequencies of the detector can, in fact, be expressed as

$$|\gamma_0| = T_{\text{corr}}/T_{\text{bar}} \quad (26)$$

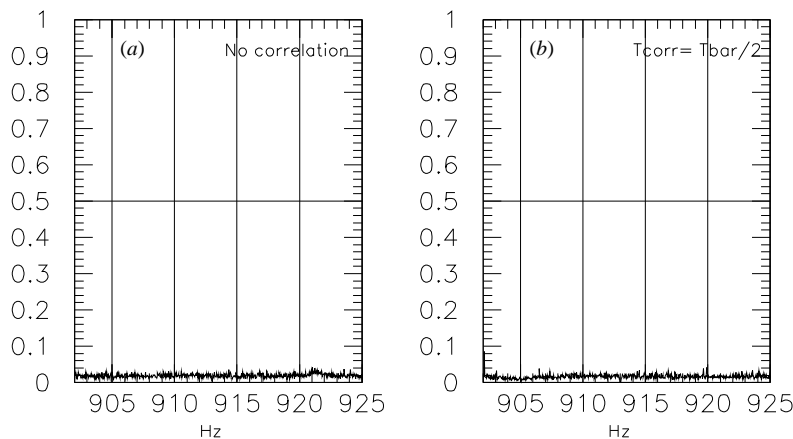


Figure 6. Simulation. Modulus of the imaginary part of the coherence function: (a) without correlation; (b) with partial correlation ($T_{\text{corr}} = T_{\text{bar}}/2$).

for two identical antennas. The results are shown in figure 5 for the absolute values of the real part of $\gamma_0(f)$ and in figure 6 for the absolute imaginary part, having considered $T_{\text{corr}}/T_{\text{bar}} = 1/2$, for the frequency range that includes both resonances.

We notice values of $\gamma_0(f)$ different from zero only for the real part, as the imaginary part would give values different from zero just in the cases where the correlation is time-shifted. For the real part we notice $\gamma_0(f) = 1$ at the frequency where we have applied a calibration signal. Then we observe values different from zero at all frequencies and in particular at the resonances, where the detector has the largest sensitivity. We can compare the values of T_{corr} determined with this method, making use of (26), with those belonging to the correlated signal we have put in the simulated data for the two antennas for various values of $T_{\text{corr}}/T_{\text{bar}}$. We obtain the following table.

Table 1.

$T_{\text{corr}}/T_{\text{bar}}$ simulated	$T_{\text{corr}}/T_{\text{bar}}$ determined from the simulated data
0	0.02 ± 0.02
0.40	0.38 ± 0.03
0.50	0.49 ± 0.03
0.67	0.69 ± 0.03

In the above table the standard error has been calculated from (25) for $t_m = 36$ h and $\delta f = 33.5$ mHz multiplied by $\sqrt{\pi/2}$ because we have considered absolute values (if x and y are Gaussian variables with zero mean and standard deviation σ , then the expected value for $\sqrt{x^2 + y^2}$ is $\sigma\sqrt{\pi/2}$. The expected value for $|x|$ and $|y|$ is $\sigma\sqrt{2/\pi}$). From the simulation we get a standard deviation of 1.5×10^{-2} and 1.4×10^{-2} for the real and imaginary parts, respectively. Thus the standard deviation for the absolute value is $1.45 \times 10^{-2}\sqrt{\pi/2} = 0.018$, in agreement with the calculation. Finally, the expected value of γ_0 for $T_{\text{corr}}/T_{\text{bar}} = 0$ is just 0.018, as found by simulation.

It is possible, in general, to relate the correlated signals with a GW stochastic background. From equations (1), (8) and (21) we get

$$\Omega(920 \text{ Hz}) = \Omega_1 \frac{T}{0.1 \text{ K}} \text{Re}[\gamma_0] = \Omega_1 \frac{T_{\text{corr}}}{0.1 \text{ K}} \quad (27)$$

where

$$\Omega_1(920 \text{ Hz}) = 3.3 \left(\frac{100 \text{ km s}^{-1} \text{ Mpc}^{-1}}{H} \right)^2 \frac{2300 \text{ kg } 10^7}{M Q}.$$

T_{corr} can be read directly from a graph as in figure 5.

The standard error associated with this measurement is

$$\delta\Omega(f) \leq \frac{\Omega_1(f)(T/0.1 \text{ K}) + \Omega(f)}{\sqrt{t_m Df}}. \quad (28)$$

With one year of operation and $Df \simeq 100 \text{ Hz}$, which is within the grasp of present technology, we get $\delta\Omega \simeq 6 \times 10^{-5}$, near to the limit (ten times) calculated on the basis of nucleosynthesis considerations. An additional increase in the mass of the resonant detector by a factor of 100 and further cooling of the resonant detector will improve the sensitivity such as to make it possible to measure values as small as $\Omega(f) \simeq 10^{-7}$, which is close to the theoretical predictions of string theory [2].

6. Discussion and conclusions

Resonant GW antennas have been originally conceived, designed and optimized for short-burst detection. Their sensitivity has therefore been expressed, most of the time, in terms of the effective temperature T_{eff} , which is the minimum energy delivered by a GW burst that can be detected by the apparatus, or the corresponding pulse amplitude h . For studying the operation of a resonant antenna as a detector for a GW stochastic background we have to deal with noise spectra. This has brought us to reconsider the sensitivity to bursts and other types of GW in a somewhat different manner, which improves our understanding of the role played by the transducer and the electronics, the coupling between the bar and transducer and the other basic parameters of the apparatus. The noise spectrum of the apparatus is expressed by equation (7), which also gives the sensitivity for the GW background directly. We notice that the optimum sensitivity is obtained at the resonance (or at the resonances) and depends essentially on the ratio T_e/MQ , for a given material. The transducer and electronics determine in practice only the bandwidth of the apparatus, given by (10), with no appreciable effect on the sensitivity at resonance. To have a larger bandwidth (that is a good transducer) is consequently less important when the scientific objective is aimed at the measurement of a stochastic background. While for bursts the sensitivity expressed in terms of h depends on Δf , as shown by equation (12), the spectral amplitude (in units of $\text{Hz}^{-1/2}$) for the stochastic background depends on $Df^{1/4}$ only when cross-correlating two antennas, as shown by equation (21). For this reason it could also be convenient, in terms of cost and feasibility, to consider [22] a cross-correlation experiment between an interferometer and a nearby bar, as the greater bandwidth of the interferometer plays a minor role for the stochastic background measurements. We would like to conclude that resonant detectors, by their nature of being resonant, are particularly suited for detecting a possible GW stochastic background.

References

- [1] Thorne K S 1987 *300 Years of Gravitation* ed S W Hawking and W Israel (Cambridge: Cambridge University Press)
- [2] Brustein R, Gasperini M, Giovannini M and Veneziano G 1995 Relic gravitational waves from string cosmology *Phys. Lett.* **361B** 45
- [3] Astone P et al 1993 Long-term operation of the Rome Explorer cryogenic gravitational wave detector *Phys. Rev. D* **47** 362
- [4] Geng Z K, Hamilton W O, Johnson W W, Mauceli E, Merkowitz S, Morse A and Solomonson N 1994 Operation of the Allegro detector at LSU *Proc. 1st Edoardo Amaldi Conf. on Gravitational Wave Experiments (Rome)* ed E Coccia, G Pizzella and F Ronga (Singapore: World Scientific)
- [5] Blair D G, Heng I S, Ivanov E N, van Kann F, Linthorne N P, Tobar M E and Turner P J 1994 Operation of the Perth cryogenic resonant-bar gravitational wave detector *Proc. 1st Edoardo Amaldi Conf. on Gravitational Wave Experiments (Rome)* ed E Coccia, G Pizzella and F Ronga (Singapore: World Scientific)
- [6] Astone P, Pallottino G V and Pizzella G 1996 Detection of impulsive, monochromatic and stochastic gravitational waves with resonant antennas *Internal report Frascati, LNF-96/001 (IR)*
- [7] Pallottino G V and Pizzella G 1981 Matching of transducers to resonant gravitational-wave antennas *Nuovo Cimento C* **4** 237
- [8] Pizzella G 1975 Gravitational-radiation experiments *Nuovo Cimento C* **5** 369
- [9] Papoulis A 1984 *Probability, Random Variables, and Stochastic Processes* (Singapore: McGraw-Hill)
- [10] Pizzella G 1979 Optimum filtering and sensitivity for resonant gravitational wave antennas *Nuovo Cimento C* **2** 209
- [11] Pallottino G V and Pizzella G 1984 Sensitivity of a Weber type resonant antenna to monochromatic gravitational waves *Nuovo Cimento C* **7** 155
- [12] Hough J, Pugh J R, Bland R and Drever R W 1975 Search for continuous gravitational radiation *Nature* **254** 498
- [13] Zimmerman R L and Hellings R W 1980 Gravitational radiation dominated cosmology *Astrophys. J.* **241** 475
- [14] Compton K, Nicholson D and Schutz B F 1994 Stochastic gravitational wave background (<http://www.astro.cf.ac.uk/group/relativity/papers/abstracts/kath94a.html>) *Proc. 7th Marcel Grossman Meeting* to appear
- [15] Astone P et al 1996 Upper limit for a gravitational wave stochastic background measured with the Explorer and Nautilus gravitational wave resonant detectors *Phys. Lett.* **385B** 421
- [16] Michelson P F 1987 On detecting stochastic background gravitational radiation with terrestrial detectors *Mon. Not. R. Astron. Soc.* **227** 933
- [17] Bendat J S and Piersol A G 1966 *Measurement and Analysis of Random Data* (New York: Wiley)
- [18] Astone P et al 1994 The Nautilus experiment *Proc. 1st Edoardo Amaldi Conf. on Gravitational Wave Experiments (Rome)* ed E Coccia, G Pizzella and F Ronga (Singapore: World Scientific)
- [19] Astone P et al 1997 The gravitational wave detector NAUTILUS: apparatus and initial tests *Astropart. Phys.* at press
- [20] Cerdonio M et al 1994 Status of the Auriga gravitational wave antenna *Proc. 1st Edoardo Amaldi Conf. on Gravitational Wave Experiments (Rome)* ed E Coccia, G Pizzella and F Ronga (Singapore: World Scientific)
- [21] Astone P, Frasca S, Pallottino G V and Pizzella G 1997 The fast matched filter for gravitational wave data analysis: characteristics and applications *Nuovo Cimento* at press
- [22] Astone P, Lobo J A and Schutz B F 1994 Coincidence experiments between interferometric and resonant bar detectors of gravitational waves *Class. Quantum Grav.* **11** 2093